Raman scattering spectra in mixed $Ga_{1-x}Al_xAs(Sb)$ crystals

D. N. Talwar*
Department of Physics, University of Houston, Central Campus, Houston, Texas 77004

M. Vandevyver
Centre d'Etudes Nucleaires de Saclay, SES-Laboratoire d'Etudes et de Recherches Avancées, B. P. No.-2, 91190 Gif-sur-Yvette, France

M. Zigone
Laboratoire de Physique des Solides, de l'Université P. et M. Curie, Associe au Centre National de la Recherche Scientifique 4, Place Jessieu 75230 Paris-Cedex 05, France

(Received 11 August 1980)

A simplified Green's-function treatment is reported to explain the recent Raman scattering experiments in solid solutions with the zinc-blende structure. By incorporating phonons from an eleven-parameter rigid-ion model (RIM11) fitted-neutron (GaAs, GaSb), and optical (AlAs) data, we have studied the vibrations of low concentration of point defects in mixed $Ga_{1-x}Al_xAs(Sb)$ crystals. In the absence of precise experimental results, the present phenomenological method will be useful to predict the impurity-induced structure in different Raman-active irreducible representations by assuming derivatives of the polarizability tensor as free parameters. Explicit calculations are reported for *Ga* As:Al, *Al* As:Ga, and *Ga* Sb:Al systems. A reasonable explanation for the impurity modes and the Raman structure (wherever available) by a single perturbation parameter lend justification to the reliability of phonons by RIM11. This method may be significant for checking the internal coherence of those lattice-dynamical schemes which claim a good fit to the neutron data but suffer from internal inconsistencies. The force variation results for impurities obtained from a modified random-element-isodisplacement model fitted to the optical data (two-mode behavior) are compared and discussed with the full lattice-dynamical calculations.

I. INTRODUCTION

In ionic solids, most of the harmonic theories developed in the last decade are remarkable because of their simplicity and moreover they provide good tests of their validity in explaining several phonon-assisted properties.[1–6] However, in partially ionic zinc-blende-type crystals, some of the existing lattice-dynamical models are not consistent despite their claim for good fit to the neutron data of phonon dispersions along high-symmetry directions. In order to find a reliable shell model (SM) scheme, Kunc and Bilz[7] have recently performed numerous computer experiments considering all its (SM's) seventeen ramifications: the analysis of optical experiments in different zinc-blende systems (ZBS) led them to believe that a ten-parameter overlap valence-shell model (OVSM10) is better than the most commonly employed fourteen-parameter shell model (SM14).[8] Another important outcome of their findings was that the SM14 is not suitable for its nonlinear extension to understand the phonon-assisted Raman scattering spectra.[9] The basic point that compels recognition to a lattice-dynamical scheme demands simultaneously correct eigenvalues and eigenfunctions.[1] Inelastic neutron scattering experiments are capable of obtaining both the phonon frequencies and the eigenfunctions; however, the latter are usually not measured merely to curtail considerable extra effort and valuable experimental time. In the absence of eigenfunction data, the reliability of calculated phonons can be checked using alternative methods.

Among others, the most important way to approach the subject is to understand the phonon-assisted impurity-induced optical experiments.[10–15] The new modes (gap or localized) and the spectra in the band-mode region offer a unique opportunity to study the lattice dynamics of perfect and imperfect crystals by the Green's-function technique. Such calculations will be useful to check the internal coherence of eigenvalues and eigenfunctions in the crystal lattices.

Quite recently, impurity-induced Raman scattering experiments have been reported in mixed [$Ga_{1-x}Al_xAs$ (Refs. 16–18) and $Ga_{1-x}Al_xSb$ (Refs. 19 and 20)] systems. The observed changes in the

Raman structures with the composition x have suggested that these solid solutions exhibit two-mode behavior [i.e., the optical phonons of GaAs(Sb) and AlAs(Sb) vary linearly with the composition of Al or Ga and finally result in well-defined impurity modes for their limiting concentrations]. The Al (light) impurities for $x \cong 0$ in *Ga*As(Sb) give rise to localized vibrational modes whereas for $x \cong 1$ the Ga impurities in *Al*As(Sb) provide gap modes. Furthermore, the lattice phonon results from inelastic neutron scattering techniques [GaAs, GaSb (Refs. 21 and 22)] as well as optical experiments [AlAs (Ref. 23)] have also appeared in the literature.

For Raman scattering, the only phenomenological approach to our knowledge in which the differential polarizabilities are organically built into the lattice-dynamical model, is the nonlinear extension of the SM.[24–27] However, in ionic crystals, the existing calculations with a reasonable fit to the Raman intensity data require polarizability values which are not always realistic.[24–27] Moreover, Kunc and Bilz[7] have pointed out that the nonlinear extension of the commonly used SM14 (Ref. 8) in ZBS is not possible. It is worth mentioning that the SM14 (Ref. 8) fitted neutron data also fail to explain the simultaneously observed two-impurity modes (localized and gap) by a single defect in gallium phosphide.[28] The use of cluster models in the vibrational properties of mixed systems is again not very encouraging as it predicts a number of modes more than actually observed in optical experiments.[29,30] On the other hand, the rigid-ion-model (RIM) calculations have provided a very good explanation for the two or even more impurity effects related with a single impurity by a single perturbation parameter in several ZBS.[31–34]

From these remarks, it is apparent that a safer starting point to gain physical insight from phonon-assisted Raman scattering data is to use a simplified lattice-dynamical model. In the present paper we have studied the lattice dynamics of perfect and/or imperfect zinc-blende-type crystals using the Green's-function technique and incorporating an eleven-parameter rigid-ion model (RIM11). Without imposing additional constraints in the Green's-function theory of impurity-induced Raman scattering, the motive of the present work is to find whether or not the same perturbation parameters extracted from the impurity-mode calculations provide some correspondence to the spectra observed in the band-mode region.[18] This approach will be useful for checking the internal coherence of lattice-dynamical schemes and here in application to RIM11. The calculated impurity-induced Raman intensity and the separate information of A_1-, E-, and F_2-type impurity host vibrations[35] may encourage experimentalists to undertake similar studies. The results of our calculations for the low concentration of impurities in the $Ga_{1-x}Al_xAs$ system have provided very good correspondence to the recently reported experimental data by Kim and Spitzer.[18] In the absence of sufficient Raman results in the band-mode region for the *Ga*Sb:Al system, we have interpreted our calculations in terms of the existing optical data.[36,37] Moreover, the positions of the calculated two-phonon density of states for GaSb (both additive and subtractive) when compared with the Raman experiments[20,36,37] has provided additional justification to the accuracy of phonons by RIM11. The concentration dependence of long-wavelength optical phonons in $Ga_{1-x}Al_xAs(Sb)$ systems have also been studied in terms of the random-element-isodisplacement (REI) model of Gorska and Nazarewicz.[38] The results of force variation due to point defects obtained from the REI model are discussed with those obtained from the full lattice-dynamical treatment.

The paper is organized into five sections. The underlying physics for the impurity-induced Raman scattering in polar crystals and here in application to zinc-blende-type crystals is outlined in terms of Green's-function formulation in Sec. II. Group-theoretic arguments to simplify the problem are given, especially to obtain the relevant expressions for the components of individual impurity-induced Raman scattering intensities in Sec. III. Numerical computations are made and the results for the lattice dynamics in perfect and/or imperfect $Ga_{1-x}Al_xAs(Sb)$ systems have been compared and discussed with the existing experimental data in Sec. IV with the concluding remarks presented in Sec. V.

II. GREEN'S-FUNCTION REPRESENTATION OF LATTICE DYNAMICS

A. Perfect crystals

A comprehensive account of the dynamical properties of crystal lattices has been discussed in several review articles,[6] monographs,[2,3] and books.[1,4,39] In most of the physical situations, the method of Green's functions has become fairly standard although unnecessarily powerful and clumsy in some applications but very elegant in its formal generality. The Green's-function representation of lattice dynamics given here is general and is restricted to some of the formal results needed for understanding the impurity-induced Raman scattering spectra in zinc-blende-type crystals.

Following Maradudin *et al.*,[6] the classical Green's function for the vibrating system in matrix notation is defined as

$$\left[\underline{M}\frac{d^2}{dt^2}+\underline{\phi}\right]\underline{G}(t)=-\delta(t)\underline{I}\ , \tag{1}$$

where $\underline{M}$, $\underline{\phi}$, and $\underline{G}$ are, respectively, the mass, po-

tential energy, and Green's-function matrices and $\underline{I}$ is a unit matrix.

If a set of basis vectors that corresponds to a unit displacement along the α direction for the κth atom in the lth unit cell is defined as $|l\kappa\alpha\rangle$ then it follows that

$$\langle l\kappa\alpha|l'\kappa'\beta\rangle = \delta_{ll'}\delta_{\kappa\kappa'}\delta_{\alpha\beta} \ . \tag{2}$$

Also the displacement $\vec{u}$ for the atom $l\kappa$ along α will be denoted as $\langle l\kappa\alpha|\vec{u}\rangle$. The elements of the Green's function $\langle l\kappa\alpha|\underline{G}(t)|l'\kappa'\beta\rangle$ in Eq. (1) represent the displacement of atom $l\kappa$ along α direction due to the force $-\delta(t)$ on the atom $l'\kappa'$ in the β direction.

The Fourier transform of $\underline{G}(t)$ may be easily seen to satisfy

$$\underline{G}^{-1}(\omega) = \underline{M}\omega^2 - \underline{\phi} \ , \tag{3a}$$

or

$$[\underline{M}^{1/2}\underline{G}(\omega)\underline{M}^{1/2}]^{-1} = \underline{I}\omega^2 - \underline{D} \ , \tag{3b}$$

where $\underline{D} = \underline{M}^{-1/2}\underline{\phi}\underline{M}^{-1/2}$ is called the dynamical matrix.

The complexity of Eqs. (3a) and (3b) for evaluating $\underline{G}(\omega)$ requires a transformation of $\langle l\kappa\alpha|\vec{u}\rangle$ to a representation that diagonalizes Eq. (3a). From the elementary theory of lattice dynamics, the required transformation for periodic lattices is

$$\langle l\kappa\alpha|\vec{q}j\rangle = N^{-1/2}e_\alpha^*(\kappa|\vec{q}j)\exp[-i\vec{q}\vec{x}(l\kappa)] \ , \tag{4}$$

where $\vec{q}$ forms a set of N wave vectors in the first Brillouin zone, j is the polarization index ($1 \leq j \leq 3r$, where r is the number of atoms in the unit cell), $\vec{x}(l\kappa)$ is the equilibrium position vector of atom $l\kappa$, and $e_\alpha(\kappa|\vec{q}j)$ form the components of the polarization vector for the mode $(\vec{q}j)$ which are orthonormal

$$\sum_{\alpha\kappa} e_\alpha^*(\kappa|\vec{q}j)e_\alpha(\kappa|\vec{q}j') = \delta_{jj'} \ , \tag{5a}$$

and complete

$$\sum_j e_\alpha(\kappa|\vec{q}j)e_\beta^*(\kappa'|\vec{q}j) = \delta_{\alpha\beta}\delta_{\kappa\kappa'} \ . \tag{5b}$$

If the transformation [Eq. (4)] is used it yields

$$\langle \vec{q}j|\underline{G}(\omega)|\vec{q}'j'\rangle = [\omega^2 - \omega^2(\vec{q}j)]^{-1}\delta_{\vec{q}\vec{q}'}\delta_{jj'} \ , \tag{6}$$

where $\omega(\vec{q}j)$ is the phonon frequency of the mode $(\vec{q}j)$.

The component form of the perfect lattice Green's function in the site representation can be obtained from Eqs. (4) and (6)

$$\begin{aligned}\langle l\kappa\alpha|\underline{G}(\omega)|l'\kappa'\beta\rangle &= \frac{1}{(M_\kappa M_{\kappa'})^{1/2}N}\sum_{j\kappa} e_\alpha(\kappa|\vec{q}j)e_\beta^*(\kappa'|\vec{q}j) \\ &\quad\times\langle\vec{q}j|\underline{G}(\omega)|\vec{q}j\rangle \\ &\quad\times\exp\{i\vec{q}[\vec{x}(l\kappa)-\vec{x}(l'\kappa')]\} \ .\end{aligned} \tag{7}$$

The above Green's-function treatment is useful not only for expressing many of the vibrational properties of perfect crystalline solids but also for imperfect systems too.

B. Impurity-induced Raman scattering spectra in solids

The effect of impurities in polar cyrstals is to change the dependence of the electronic polarizability P with the atomic displacements. The polarizability may couple with the incident radiation E and can give rise to the nature of impurity-induced Raman scattering. Following Born and Huang,[39] the scattering intensity for an imperfect crystal may be expressed as

$$I(\omega_s) = \frac{\omega_i^4}{2\pi C^3}\sum_{\substack{\alpha\beta \\ \alpha'\beta'}} n_\alpha n_{\alpha'}E_\beta E_{\beta'}\, i_{\alpha\beta\alpha'\beta'}(\Delta\omega) \ , \tag{8}$$

where n_α is the α component of a unit polarization vector parallel to the scattered light, E_β is the β component of the incident field, ω_i and $\omega_s (\equiv \omega_i + \Delta\omega)$ are the frequencies of the incident and scattered light. In the Green's-function matrix notation, the tensor $\underline{i}(\omega)$ for the first-order impurity-induced Raman scattering process is

$$\begin{aligned}i_{\alpha\beta\alpha'\beta'}(\omega) = \rho\frac{\hbar}{\pi}\sum_{\substack{l\kappa \\ l'\kappa' \\ \mu\nu}}\eta(\omega)\frac{\partial P_{\alpha\beta}}{\partial u_{l\kappa\mu}} \\ \times \mathrm{Im}\langle l\kappa\mu|\underline{U}(\omega)|l'\kappa'\nu\rangle\frac{\partial P_{\alpha'\beta'}}{\partial u_{l'\kappa'\nu}} \ ,\end{aligned} \tag{9}$$

where

$$\eta(\omega) = \begin{cases}[1-\exp(-x)]^{-1}, & \omega > 0, \text{ Stokes process} \\ [\exp(x)-1]^{-1}, & \omega < 0, \text{ anti-Stokes process}\end{cases}$$

$$\text{with } x = \frac{\hbar\omega}{k_B T}$$

and ρ is the concentration of impurities.

The imperfect Green's function $\underline{U}(\omega)$ in Eq. (9) is related to $\underline{G}(\omega)$ and the perturbation matrix $\delta\underline{L}(\omega)$ by the well-known Dyson's equation as

$$\begin{aligned}\underline{U}(\omega) &= \underline{G}(\omega)[\underline{I} - \delta\underline{L}(\omega)\underline{G}(\omega)]^{-1} \\ &= [\underline{I} - \underline{G}(\omega)\delta\underline{L}(\omega)]^{-1}\underline{G}(\omega) \ .\end{aligned} \tag{10}$$

Furthermore, the first-order derivative of the polarizability $(\partial P/\partial u)$ tensor, which governs the excitation or deexcitation of the one-phonon Raman process in the expansion

$$P_{\alpha\beta} = P_{\alpha\beta}^0 + \sum_{l\kappa\gamma}\frac{\partial P_{\alpha\beta}}{\partial u_{l\kappa\gamma}}\langle l\kappa\gamma|\vec{u}\rangle + \cdots \tag{11}$$

has been retained in Eq. (9) as $P_{\alpha\beta}^0$ is zero in cubic crystals.

III. GROUP-THEORETIC ANALYSIS

In the case of low concentration of isoelectronic-point defects in ZBS, the effect of impurities can be assumed to be significant only up to their first-nearest neighbors. With this assumption and using group-theoretic arguments, the problem of impurity vibrations becomes easily tractable. Since the displacement coordinates of the first-nearest neighbors form a basis for a reducible representation, it is convenient to work in the $\langle l\kappa\alpha|\Gamma_i\rangle$ representation of the normalized symmetry coordinates pertaining to the point group T_d. Here Γ is each one of the irreducible representations contained in the perturbation and i refers to the ith partner function of Γ. Furthermore, only those irreducible representations are said to be *Raman active* in which the tetrahedral molecule (e.g., $GaAs_4$) related with the nearest-neighbor coordinates in the GaAs lattice (for example) suffer internal distortions while those in which the molecule moves as a rigid unit will be *Raman inactive*.[35,40]

If the derivatives of the polarizability tensor, which are very-little-known quantities vanishing in terms of harmonic approximation are considered as free parameters, the scattering tensor for each of the Raman-active (A_1, E, and F_2) irreducible representations can be calculated for point defects in zinc-blende-type crystals as [using Eqs. (8) and (9)]

$$I(A_1) \cong C^2(A_1)\,\mathrm{Im}\langle\Gamma_{A_1}|\underline{U}|\Gamma_{A_1}\rangle \ ,$$

$$I(E) \cong C^2(E)\,\mathrm{Im}\langle\Gamma_E|\underline{U}|\Gamma_E\rangle \ ,$$

and

$$\begin{aligned} I(F_2) \cong\ & C^2(F_2^a)\,\mathrm{Im}\langle\Gamma_{F_2^a}|\underline{U}|\Gamma_{F_2^a}\rangle \\ & + 2C(F_2^a)C(F_2^b)\,\mathrm{Im}\langle\Gamma_{F_2^a}|\underline{U}|\Gamma_{F_2^b}\rangle \\ & + C^2(F_2^b)\,\mathrm{Im}\langle\Gamma_{F_2^b}|\underline{U}|\Gamma_{F_2^b}\rangle \ , \end{aligned} \tag{12}$$

where $C(A_1)$, $C(E)$, . . . , etc., are the unknown parameters related with the derivative of the polarizability to the atomic displacements. For each of the A_1- and E-type vibrations, $C(A_1)$ and $C(E)$ create absolutely no problem as they will merely scale the intensity curves. For F_2-type vibrations the constant $C(F_2^a)$ is related with the relative movements of cation and anion along the threefold axis where as $C(F_2^b)$ is related with stretching and compression along the same direction in the case of a fixed center. In the absence of precise experimental results, one may also treat $C(F_2^a)/C(F_2^b)$ as a free parameter. The relevant forms of the Green's function $\underline{G}$, and the perturbation matrix $\underline{\delta L}$ belonging to various Raman-active irreducible representations have been given in Table I.

TABLE I. Green's function and perturbation matrices in the Raman-active irreducible representations for a substitutional point defect in zinc-blende-type crystals: the terms ($g_1^{\pm}, g_2^{\pm}, \ldots, g_8^{\pm}$) are the nonzero Green's-function matrix elements in the nearest-neighbor impurity host cage (see Ref. 31); A, B, are the nearest-neighbor force constants in the RIM and t stands for the force variation parameter in the notations of Ref. 32; (+) and (−) signs correspond to the cation and anion, respectively, while M' represents the mass of the impurity atom.

$G(\omega)$ matrix	Γ_{A_1}	Γ_E	$\Gamma_{F_2^a}$	$\Gamma_{F_2^b}$	$\Gamma_{F_2^c}$
Γ_{A_1}	$(g_2^{\pm}-2g_5^{\pm}+g_6^{\pm}-2g_7^{\pm}+4g_8^{\pm})$	. . .	. . .	. . .	. . .
Γ_E	. . .	$(g_2^{\pm}-2g_5^{\pm}+g_6^{\pm}+g_7^{\pm}-2g_8^{\pm})$	. . .	. . .	. . .
$\Gamma_{F_2^a}$	. . .	. . .	$\frac{1}{5}(g_2^{\pm}+4g_1^{\pm}-8g_3^{\pm}+2g_5^{\pm}+g_6^{\pm})$	$\sqrt{2/5}\,(g_7^{\pm}-4g_4^{\pm})$	$\frac{2}{5}(g_2^{\pm}-g_1^{\pm}-3g_3^{\pm}+g_6^{\pm}+2g_5^{\pm})$
$\Gamma_{F_2^b}$	. . .	. . .	$\sqrt{2/5}(g_7^{\pm}-4g_4^{\pm})$	$(g_2^{\pm}-g_6^{\pm}-g_7^{\pm}-2g_8^{\pm})$	$2\sqrt{2/5}\,(g_4^{\pm}+g_7^{\pm})$
$\Gamma_{F_2^c}$	. . .	. . .	$\frac{2}{5}(g_2^{\pm}-g_1^{\pm}-3g_3^{\pm}+g_6^{\pm}+2g_5^{\pm})$	$2\sqrt{2/5}\,(g_4^{\pm}+g_7^{\pm})$	$\frac{1}{5}(g_1^{\pm}+4g_2^{\pm}+8g_3^{\pm}+4g_5^{\pm}+4g_6^{\pm})$
$\delta L(\omega)$ matrix					
Γ_{A_1}	$(A+2B)t$	. . .	. . .	. . .	. . .
Γ_E	. . .	$(A-B)t$	. . .	. . .	. . .
$\Gamma_{F_2^a}$	. . .	. . .	$\frac{4}{5}\omega^2(M_{\pm}-M'_{\pm})+5At$	$\sqrt{10}\,Bt$	$-\frac{2}{5}\omega^2(M_{\pm}-M'_{\pm})$
$\Gamma_{F_2^b}$	. . .	. . .	$\sqrt{10}\,Bt$	$(A+B)t$	0
$\Gamma_{F_2^c}$	. . .	. . .	$-\frac{2}{5}\omega^2(M_{\pm}-M'_{\pm})$	0	$\frac{1}{5}\omega^2(M_{\pm}-M'_{\pm})$

TABLE II. Calculated force variation due to point defects in Ga-Al compounds.

System	Localized/or gap mode (cm^{-1})	Relative force variation f^a	b
Ga As:Al	359[c]	0.18	0.098
Al As:Ga	252[c]	0.23	−0.11
Ga Sb:Al	315[d]	−0.15	0.109
Al Sb:Ga	≃212[d]	. . .	−0.122

[a]Present study.
[b]REI model (from Table III).
[c]Reference 18.
[d]Reference 19.

IV. NUMERICAL COMPUTATIONS, RESULTS AND DISCUSSIONS

A. Impurity-induced first-order Raman scattering

It has been pointed out that the use of RIM for calculating the Raman scattering intensities is not adequate because of the neglect of polarizability of ions. However, if the derivatives of the polarizability tensor are considered as unknown parameters, the nature of impurity-induced Raman scattering intensities can be understood. This approach is similar to that described and used in the literature for point defects in alkali[41] and cesium halides.[42]

The lattice phonons (eigenvalues and eigenfunctions) and thereby the relevant lattice Green's functions are computed using RIM11 (Ref. 43) by fitting the available neutron scattering [GaAs (Ref. 21) and GaSb (Ref. 22)] and optical [AlAs (Ref. 23)] data. A simplified perturbation model,[32] that accounts for the change of the nearest-neighbor coupling constant as well as the mass change at the impurity site, is considered to extract information regarding the force variations incurred in *Ga* As(Sb):Al and *Al* As:Ga systems (see Table II). Using these parameters together with Eq. (12), the Raman structures for different impurity-host vibrations are calculated. In order to have some correspondence with the experimental structure, we have plotted the imaginary part of the imperfect Green's functions projected in the spaces of Raman-active (A_1, E, and F_2) irreducible representations.

Individual results

a. $Ga_{1-x}Al_xAs$ system. The long-wavelength optical phonons in the $Ga_{1-x}Al_xAs$ system display two-mode behavior, a property that has been studied in the past few years both by ir (Ref. 44) and Raman spectroscopy.[16–18] More recently Kim and Spitzer[18] have provided confirmation to the mode behavior and reported additional Raman structures for the acoustical vibrations too. In the limiting values of x, the results of Kim and Spitzer[18] can be understood in terms of our calculations. For the lowest value of x, the experimental structure has been displayed in Fig. 1(a) and compared with the calculated individual Raman-active components [cf. Fig. 1(b)]. A very good

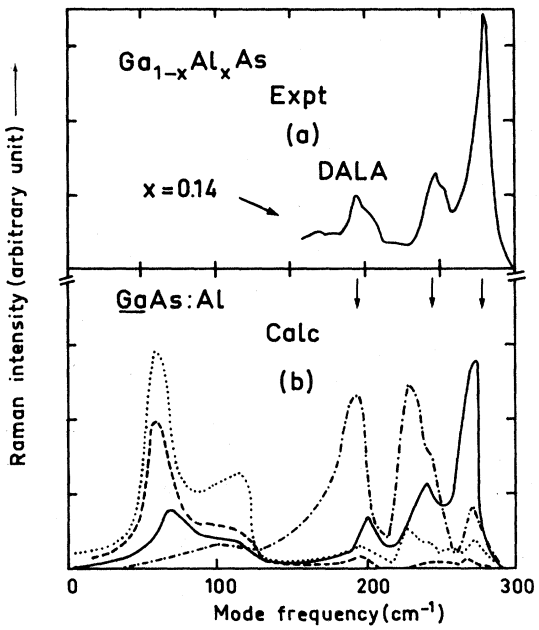

FIG. 1. Calculated Raman scattering intensity in *Ga* As:Al system using the perturbation parameter as given in Table I. The curve (a) represents the experimental data by Kim and Spitzer (Ref. 18) whereas in (b) we have plotted the individual contributions of A_1, E, and F_2 type of representations to the scattering intensity: A_1(−·−·), E(· · · ·), F_2^a(——), and F_2^b(− − −). The vertical arrows in the lower part are a guide to the eye for a quick comparison of the experimental structure with the calculated one in the F_2^a irreducible representation.

correspondence with the experimental results including the defect-activated longitudinal-acoustic (DALA) peak with the calculated structure in the F_2^q-irreducible representation can be easily marked.

When the molar concentration of Al constituents is increased (i.e., for $x \rightarrow 1$), Tsu *et al.*,[16] have suggested a well-defined gap mode ($\cong 252$ cm^{-1}) and a DALA peak ($\cong 197$ cm^{-1}) related with the vibration of Ga impurities in the AlAs lattice by Raman spectroscopy. In Fig. 2(a) the sum of the Raman structures calculated for *Al*As:Ga in the $(A_1 + E + F_2^q)$ irreducible representations is shown while in Fig. 2(b) the individual components for the impurity-host vibrations are plotted. We find that the position of the gap mode ($\cong 252$ cm^{-1}) lies exactly within the region where the calculated one-phonon density of states ($\cong 237$–330 cm^{-1}) is zero and a peak near 197 cm^{-1} also corresponds well with the experimental results of Tsu *et al.*[16]

b. $Ga_{1-x}Al_xSb$ system. The Raman experiments[19,20] performed in recent years for $Ga_{1-x}Al_xSb$ system are mostly aimed to understand the optical-mode behavior, consequently these experiments are confined to the region near $\vec{q} \cong 0$. As two-mode behavior is confirmed, the occurrence of localized (*Ga*Sb:Al) and gap (*Al*Sb:Ga) modes has been well established. Unfortunately, the impurity-induced Raman data in the band-mode region is still lacking, moreover there do not exist neutron scattering results of phonon dispersions for AlSb. We have therefore predicted the structures for impurity-host vibrations for the *Ga*Sb:Al system in Fig. 3. Since the aluminium impurities in gallium antimonide are not going to appreciably affect the band modes, then all the features found in the calculated one-phonon density of states will be reflected in the Raman structure too. In the absence of detailed experimental results, especially the variation of LA(L) mode with the impurity concentration (x) in $Ga_{1-x}Al_xSb$ system, it is not wise to unambiguously assign the structure near 148 cm^{-1} as a DALA peak (see Fig. 4 too).

In order to compare the positions of various van Hove singularities arising from a pair of phonons in GaSb we have also calculated the two-phonon additive and subtractive density of states (cf. Fig. 5). It is fair to mention that in recent years, the calculated *one*-phonon density of states with its frequency scale expanded by a factor of *two* has been used to correlate the second-order Raman spectrum in various ele-

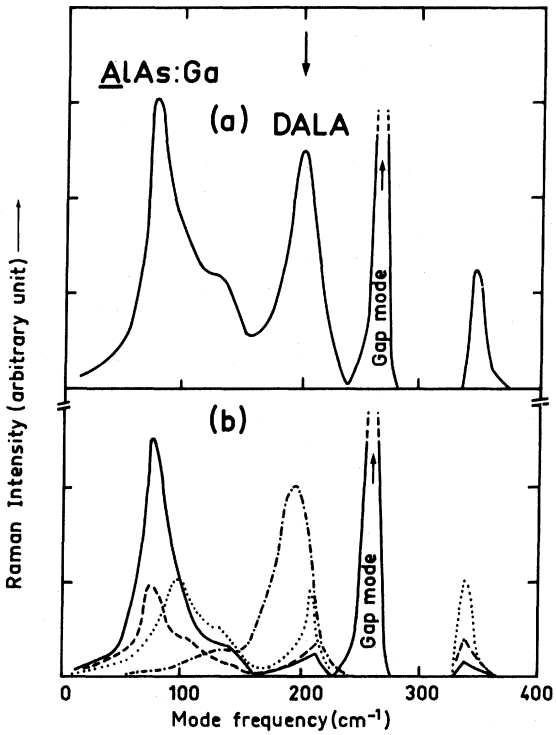

FIG. 2. Calculated Raman structure in *Al*As:Ga system using the perturbation parameter as given in Table I. The curve (a) represents the sum of structures in $(A_1 + E + F_2^q)$ irreducible representations whereas in (b) the individual contributions of A_1, E, and F_2 type of irreducible representations to the scattering intensity are plotted: A_1(–·–·), E(· · · ·), F_2^q(——), and F_2^b(– – –). The vertical arrows represent the positions of the DALA and gap modes as suggested by Tsu *et al.* (Ref. 16).

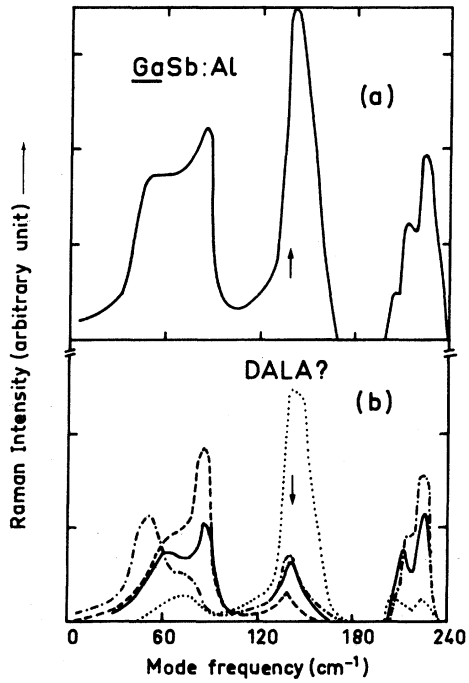

FIG. 3. Same key as Fig. 2 but for the *Ga*Sb:Al system.

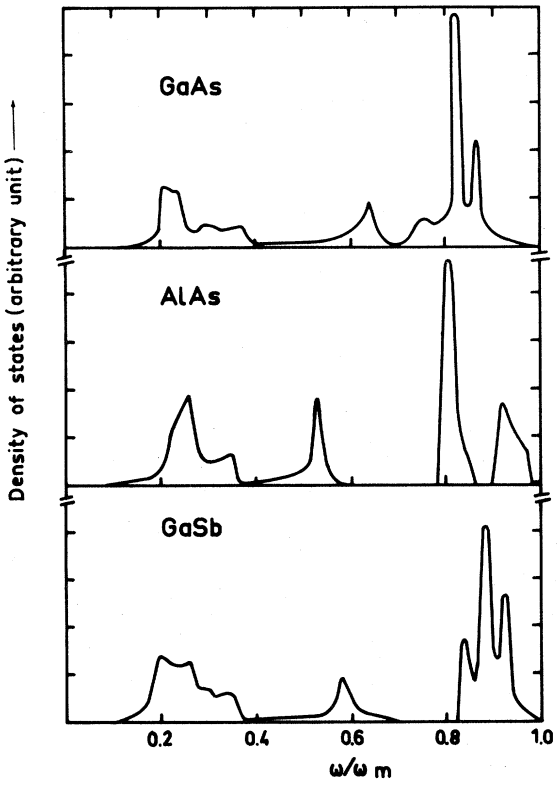

FIG. 4. Calculated one-phonon density of states by RIM11 for GaAs, AlAs, and GaSb systems. The existing gap for AlAs and GaSb lie in the frequency regions 237–330 and 168–202 cm^{-1}, respectively.

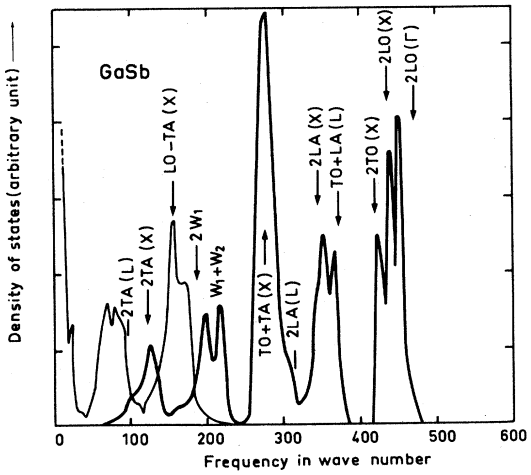

FIG. 5. Calculated two-phonon density of states (—— additive) (—— subtractive) for GaSb in terms of RIM11. The arrows marked correspond to the positions of the Raman structure observed by Klein and Chang (Ref. 36) and Charfi *et al.* (Ref. 37).

mental[44,45] and compound semiconductors[46–48] [including GaSb (Ref. 36)]. Since most of the combination bands [e.g., TO+TA(X), LO+LA(X), etc.] may contribute to the Raman spectrum, however, one cannot find their correspondence in the scaled one-phonon density of states. From Fig. 5, one may note that the positions of the Raman structure[36] observed in experimental measurements (marked by arrows) correspond very well with the calculated two-phonon density of states. Furthermore, we have made a tentative assignment of the additive and subtractive peaks considering their characteristic temperature dependence[49] and using polarization selection rules[50] (cf. Fig. 5).

B. Optical phonons in mixed $Ga_{1-x}Al_xAs(Sb)$ systems

The behavior of long-wavelength optical phonons in mixed crystals has been well interpreted in terms of a random-element-isodisplacement model[51] and its various ramifications.[52–54] By including the concept of effective electric field, Gorska and Nazarewicz[38] have made a precise modification in the REI method. Using the same theory, we report here the results of our calculations for the concentration dependence of long-wavelength optical phonons in $Ga_{1-x}Al_xAs(Sb)$ systems (cf. Fig. 6) with the parameter values given

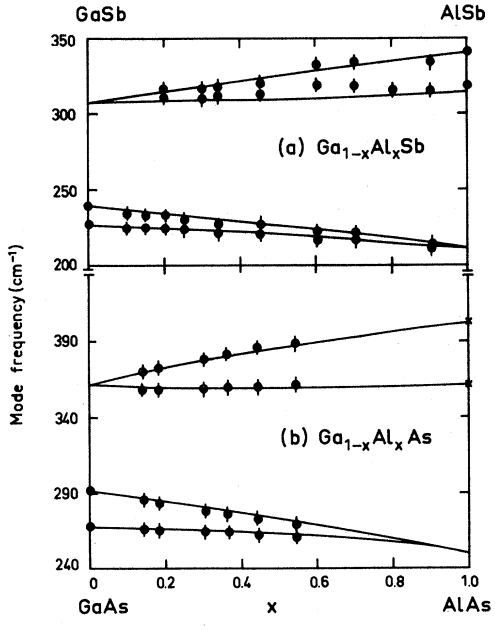

FIG. 6. The calculated fit of the concentration dependence of the optical phonons in mixed $Ga_{1-x}Al_xSb$ and $Ga_{1-x}Al_xAs$ systems using the random-element-isodisplacement model of Gorska and Nazarewicz (Ref. 38). The experimental points (♦ ∗) are taken from Biryulin *et al.* (Ref. 19) for $Ga_{1-x}Al_xSb$ and from Kim and Spitzer (Ref. 18) for $Ga_{1-x}Al_xAs$, respectively.

TABLE III. Values of the parameters used in the REI model of Gorska and Nazarewicz (Ref. 38) for fitting the concentration dependence of the optical modes of $Ga_xAl_{1-x}As(Sb)$ systems (see Fig. 6). $A_xB_{1-x}C$ with A = Ga, B = Al, C = As(Sb).

Parameters	$Ga_xAl_{1-x}As$[a]	$Ga_xAl_{1-x}Sb$[b]
$AC_{\omega_{LO}(\Gamma)}$	292 cm^{-1}	241 cm^{-1}
$AC_{\omega_{TO}(\Gamma)}$	268 cm^{-1}	226 cm^{-1}
ω_{loc}	359 cm^{-1}	$\simeq$ 307 cm^{-1}, 316 cm^{-1}
AC_{ϵ_∞}	10.9	14.4
$BC_{\omega_{LO}(\Gamma)}$	404 cm^{-1}	340 cm^{-1}
$BC_{\omega_{TO}(\Gamma)}$	362 cm^{-1}	319 cm^{-1}
ω_{gap}	252 cm^{-1}	$\simeq$ 212 cm^{-1}
BC_{ϵ_∞}	8.5	10.2
FACO	0.204×10^6 dyn cm^{-1}[c]	0.166×10^6 dyn cm^{-1}[c]
FBCO	0.184×10^6 dyn cm^{-1}[c]	0.148×10^6 dyn cm^{-1}[c]
FABO	0.56×10^5 dyn cm^{-1}[c]	0.19×10^5 dyn cm^{-1}[c]
e^*_{AC}	$0.51e$[c]	$0.365e$[c]
e^*_{BC}	$0.64e$[c]	$0.476e$[c]
θ	0.13[c]	0.10[c]

[a]Reference 18. [b]Reference 19. [c]Present study.

in Table III.

For mixed $A_xB_{1-x}C$ crystals, the force constants FACO (FBCO) in REI represent the nearest-neighbor interactions for AC (BC) crystals. In the limiting values of x, the trends of force variations due to impurities B (A) in AC (BC) can be approximately calculated and the results are included in Table II.

Before analyzing the trends of force variations it is necessary to point out that in REI model: (a) the three force constants (FACO, FBCO, and FABO) have the same compositional dependence, such that

$$F\alpha\beta x = F\alpha\beta O(1-\theta x) \ , \tag{13}$$

with $\alpha, \beta = A$, B, or C; and θ is a constant; (b) all the atoms of a given species vibrate in phase with identical amplitudes; and (c) the vibrational-mode frequencies due to isolated impurities B (or A) in AC (BC) are related by

$$\omega^2_{loc}(\underline{A}C{:}B) = (FABO + FBCO)/M_B \tag{14}$$

and

$$\omega^2_{gap}(\underline{B}C{:}A) = (FABO + FACO)/M_A \ , \tag{15}$$

where M_B and M_A are the masses of impurity atoms B and A, respectively.

The above expressions for the local- and gap-mode frequencies involve only the masses of the vibrating impurities while the host lattice atoms are supposed to be *frozen*. This situation is hardly realistic as the impurity modes do depend on the atomic vibrations of both the impurity and host lattice atoms. In the case of a gap mode, for example, the atom A (impurity) and C (host) vibrate in opposite phase[6] and thus the neglect of the vibrations of the host lattice atoms reflects a basic shortcoming of the REI model. Since the mobile mass involved in the actual movements is not well estimated but, moreover, is compensated by taking arbitrary values of the nearest- and next-nearest-neighbor force constants, then the discrepancy in the force variations with respect to the full lattice-dynamical treatment is not surprising. Considering these comments, we feel that further work is needed to make the simplified REI model more realistic.

V. GENERAL REMARKS AND CONCLUSIONS

As the atoms in real solids interact with each other by varied and complex forces, they provide us the opportunities to develop lattice-dynamical schemes in various ways by defining the *force field,* and, moreover, by the *art of approximations.* However, it is not simple to assess the internal coherence of a number of such calculations which claim a good fit to the neutron data (of phonon dispersions) but suffer from several internal inconsistencies. In this respect a recently reported lattice-dynamical calculation in various ZBS crystals by Kushwaha and Kushwaha[55] is worth mentioning: the authors have proposed a phenomenological scheme amenable to the calcula-

tions by adding three bond-bending forces in the five-parameter RIM (BBFM8). What is important in the present context is the contrast in their results of the density of phonons with the existing calculations.[43] Although they have found excellent fit with the neutron data of phonon dispersions along high-symmetry directions, the nonzero density of phonons in the vibrational spectra for ZnS (as they have claimed for), GaP, and InP (a small gap) is misleading.

In diatomic crystals where the masses of the two atoms are significantly different, Maradudin[6] has explained the conditions for the occurrence of zero density of phonons, and this is equally supported by various optical experiments.[10–14] In view of this simple argument, the model by Kushwaha and Kushwaha[55] suffers from a serious drawback and cannot be useful for understanding the simultaneous occurrence of localized and gap modes in ZBS crystals (e.g., *Zn*S:Be). It was mentioned earlier that, Kim and Yip[28] were also unsuccessful in explaining the two impurity modes in GaP by SM14. The inconsistencies of the phonon energies (and/or eigenfunctions) in the calculations of BBFM8 and SM14 can be attributed to the description of phenomenological parameters and, moreover, the methods adopted in their numerical evaluations. For further discussion, we refer to an earlier paper[34] and references cited therein.

Although the polarizability of ions is not included in RIM, the success for understanding two or even more impurity modes associated with a single impurity by a single perturbation parameter provides support at least of the accuracy of phonons.[31–34] Now the satisfactory description of impurity-assisted Raman structure in the band-mode region using a single perturbation parameter (in *Ga*As:Al and *Al*As:Ga systems) and a reasonable comparison with the additive and subtractive phonon-energy values for GaSb lend additional justification to the reliability of lattice vibrations by RIM11. We are planning to examine the question whether the simplified RIM or a more physically plausible ramification of shell model (OVSM10) will provide better understanding to the vibrational properties of perfect and/or imperfect zinc-blende-type crystals.

ACKNOWLEDGMENTS

We are thankful to Dr. Karél Kunc for his valuable suggestions and remarks regarding the shell-model calculations and especially for pointing out its inconsistencies. One of us (D.N.T.) is grateful to the authorities CEA Saclay for providing him an opportunity as a collaborator in their services d'Electronique de Saclay where most of the present work was completed. D.N.T. is also thankful for partial support by ONR Grant No. N00014-78-C0505 at the University of Houston, Texas.

---

*Permanent address: Department of Physics, University of Allahabad, Allahabad-211002, India.

[1]G. Venkataraman, L. A. Feldkamp, and V. C. Sahni, *Dynamics of Perfect Crystals* (MIT, Cambridge, Mass. 1975), and references cited therein.

[2]S. K. Sinha, CRC Crit. Rev. Solid State Sci. 3, 273 (1973).

[3]W. Cochran, CRC Crit. Rev. Solid State Sci. 2, 1 (1971).

[4]J. A. Reissland, *The Physics of Phonons* (Wiley-Interscience, New York, 1973).

[5]G. Venkataraman and V. C. Sahni, Rev. Mod. Phys. 42, 409 (1970).

[6]A. A. Maradudin, E. W. Montroll, C. H. Weiss, and I. P. Ipatova, in *Solid State Physics,* 2nd ed., edited by H. Ehrenreich, F. Seitz, and D. Turbull (Academic, New York, 1971), Suppl. 3; A. A. Maradudin, in *Astrophysics and the Many Body Problem, 1962 Brandeis Lectures* (Benjamin, New York, 1963), Vol. 2; A. A. Maradudin, Rep. Prog. Phys. 28, 331 (1965); in *Solid State Physics,* edited by F. Seitz and D. Turnball (Academic, New York, 1966), Vols. 18 and 19.

[7]K. Kunc and H. Bilz, Solid State Commun. 19, 1027 (1976).

[8]J. L. T. Waugh and G. Dolling, Phys. Rev. 132, 2410 (1963). For complete references of SM14 lattice dynamical calculations in zinc-blende-type crystals please see, S. Hoshino, Y. Fujii, J. Harada, and J. D. Axe, J. Phys. Soc. Jpn. 41, 965 (1976).

[9]K. Kunc (private communication).

[10]R. C. Newman, *Infrared Studies of Crystal Defects* (Taylor and Francis, London, 1973).

[11]A. Mitsuishi and A. Manabe, Oyo Butsuri 41, 7 (1972).

[12]W. G. Spitzer, in *Festkörperprobleme XI,* edited by O. Madelung (Pergamon, New York, 1971), pp. 1–44.

[13]M. V. Klein, in *Physics of Color Centers,* edited by W. G. Fowler (Academic, New York, 1968), Chap. 7, p. 429.

[14]A. S. Barker and A. J. Sievers, Rev. Mod. Phys. Suppl. 47, S1 (1975).

[15]*Localized Excitations in Solids,* edited by R. F. Wallis (Plenum, New York, 1968).

[16]R. Tsu, H. Kawamura, and L. Esaki, in *Proceedings of the International Conference on Physics of Semiconductors, Warsaw* (Elsevier, Amsterdam, 1972), Vol. 2, p. 1135; Phys. Rev. Lett. 29, 1397 (1972).

[17]A. S. Barker, J. L. Merz, and A. C. Gossard, Phys. Rev. B 17, 3181 (1978).

[18]O. K. Kim and W. G. Spitzer, J. Appl. Phys. 50, 4362 (1979).

[19]Y. F. Biryulin, G. M. Zinger, I. P. Ipatova, Y. E. Pozhidaev, and Y. V. Shamartsev, Sov. Phys. Semicond. 13, 948 (1979).

[20]F. Charfi, M. Zouaghi, A. Joullie, M. Balkanski, and Ch. Hirlimann, J. Phys. (Paris) 41, 83 (1980).

[21]G. Dolling and J. L. T. Waugh, in *Proceedings of the International Conference on Lattice Dynamics, Copenhagen,*

Denmark, 1963, edited by R. F. Wallis (Pergamon, London, 1965), p. 19.
[22]M. K. Farr, J. G. Traylor, and S. K. Sinha, Phys. Rev. B11, 1587 (1975).
[23]H. Masui, P. B. Klein, R. K. Chang, and R. H. Callender, in *Proceedings of 12th International Conference on the Physics of Semiconductors,* edited by M. H. Pilkhun (Teubner, Stuttgart, 1974), p. 509.
[24]A. D. Bruce and R. A. Cowley, Ind. J. Pure Appl. Phys. 9, 877 (1971); J. Phys. C 5, 595 (1972).
[25]H. Bilz, M. Buchananan, K. Fisher, R. Haberkorn, and U. Schröder, Solid State Commun. 16, 1023 (1975).
[26]S. Go, H. Bilz, and M. Cardona, Phys. Rev. Lett. 34, 500 (1975).
[27]R. L. Schmidt, K. Kunc, M. Cardona, and H. Bilz, Phys. Rev. B 20, 3345 (1979).
[28]C. H. Kim and S. Yip, J. Chem. Phys. 57, 4055 (1972).
[29]A. W. Verleur and A. S. Barker, Phys. Rev. 149, 715 (1966).
[30]N. D. Strahm and A. L. McWhorter, in *Proceedings of the International Conference on Light Scattering in Solids,* edited by G. B. Wright (Springer-Verlag, New York, 1969), p. 455.
[31]D. N. Talwar and Bal K. Agrawal, Phys. Rev. B 12, 1432 (1975).
[32]M. Vandevyner and P. Plumelle, Phys. Rev. B 17, 675 (1978).
[33]D. N. Talwar, M. Vandevyver, and M. Zigone, J. Phys. C 13, 3775 (1980).
[34]M. Vandevyver and D. N. Talwar, Phys. Rev. B 21, 3405 (1980).
[35]E. B. Wilson, J. C. Decius, and P. C. Cross, *Molecular Vibrations* (McGraw-Hill, New York, 1955).
[36]P. B. Klein and R. K. Chang, Phys. Rev. B 14, 2498 (1976).
[37]F. Charfi, M. Zouaghi, C. Llinares, M. Balkanski, Ch. Hirlimann, and A. Joullie, in *Proceedings of the International Conference on Lattice Dynamics,* edited by M. Balkanski (Flammaron, Paris, 1977), p. 430.
[38]M. Gorska and W. Nazarewicz, Phys. Status Solidi (b) 65, 193 (1974).
[39]M. Born and K. Huang, *Dynamical Theory of Crystal Lattices* (Oxford University Press, London, 1954).
[40]G. Herzberg, *Spectra of diatomic molecules,* 2nd ed. (Van Nostrand, New York, 1950).
[41]G. Benedek and G. F. Nardelli, Phys. Rev. 154, 872 (1967).
[42]T. P. Martin, J. Phys. C 5, 493 (1972).
[43]K. Kunc, Ann. Phys. (Paris) 8, 319 (1973).
[44]B. A. Weinstein and M. Cardona, Solid State Commun. 10, 961 (1972).
[45]B. A. Weinstein and M. Cardona, Phys. Rev. B 7, 2545 (1973).
[46]W. Kiefer, W. Richter, and M. Cardona, Phys. Rev. B 12, 2346 (1975).
[47]R. L. Schmidt, B. D. McCombe, and M. Cardona, Phys. Rev. B 11, 746 (1975).
[48]R. M. Hoff and J. C. Irwin, Phys. Rev. B 10, 3464 (1974).
[49]J. N. Hodgson, *Optical Absorption and Dispersions in Solids* (Chapman and Hall, London, 1970), p. 40.
[50]J. L. Birman, Phys. Rev. 131, 1409 (1963).
[51]Y. S. Chen, W. Shockley, and G. L. Pearson, Phys. Rev. 151, 648 (1966).
[52]I. F. Chang and S. S. Mitra, Phys. Rev. 172, 924 (1968); Adv. Phys. 20, 359 (1971).
[53]M. Illegems and G. L. Pearson, Phys. Rev. B 1, 1576 (1970).
[54]E. Jahne, Phys. Status Solidi (b) 74, 275 (1976); 75, 221 (1976).
[55]M. S. Kushwaha and S. S. Kushwaha, J. Phys. Chem. Solids 41, 489 (1980); Can. J. Phys. 58, 351 (1980); Phys. Status Solidi (b) 98, 623 (1980).